

# 1 Evaluating assembly and variant calling software 2 for strain-resolved analysis of large DNA-viruses

3  
4 Z.-L. Deng <sup>1,3</sup>, A. Dhingra <sup>2,3</sup>, A. Fritz <sup>1</sup>, J., Götting <sup>2</sup>, P. C. Münch <sup>1,4</sup>, L. Steinbrück <sup>2</sup>, T. F.  
5 Schulz <sup>2,3</sup>, T. Ganzenmüller <sup>2,3,5</sup>, A. C. McHardy\* <sup>1,3</sup>

6  
7  
8 1 Computational Biology of Infection Research, Helmholtz Centre for Infection Research,  
9 38124 Braunschweig, Germany

10 2 Institute of Virology, Hannover Medical School, Hannover, Germany

11 3 German Center for Infection Research (DZIF), Hannover-Braunschweig site, Germany

12 4 Chair of Medical Microbiology and Hospital Epidemiology, Max von Pettenkofer Institute,  
13 Faculty of Medicine, Ludwig Maximilian University of Munich, Munich, Germany

14 5 Institute for Medical Virology, University Hospital Tübingen, Tübingen, German

15

16 Corresponding author: A. C. McHardy, Department Computational Biology of Infection  
17 Research, Helmholtz Centre for Infection Research, Braunschweig, Germany

18 Email: [Alice.McHardy@helmholtz-hzi.de](mailto:Alice.McHardy@helmholtz-hzi.de)

19 Tel: +49 531 391-55271

20

21

22

23

24 **Keywords:** HCMV; strain mixtures; virus; benchmark; genome assembly; variant  
25 calling

## 1 Abstract

2 Infection with human cytomegalovirus (HCMV) can cause severe complications in  
3 immunocompromised individuals and congenitally infected children. Characterizing  
4 heterogeneous viral populations and their evolution by high-throughput sequencing of  
5 clinical specimens requires the accurate assembly of individual strains or sequence  
6 variants and suitable variant calling methods. However, the performance of most  
7 methods has not been assessed for populations composed of low divergent viral  
8 strains with large genomes, such as HCMV. In an extensive benchmarking study, we  
9 evaluated 15 assemblers and six variant callers on ten lab-generated benchmark data  
10 sets created with two different library preparation protocols, to identify best practices  
11 and challenges for analyzing such data.

12 Most assemblers, especially metaSPAdes and IVA, performed well across a range of  
13 metrics in recovering abundant strains. However, only one, Savage, recovered low  
14 abundant strains and in a highly fragmented manner. Two variant callers, LoFreq and  
15 VarScan2, excelled across all strain abundances. Both shared a large fraction of false  
16 positive (FP) variant calls, which were strongly enriched in T to G changes in a “G.G”  
17 context. The magnitude of this context-dependent systematic error is linked to the  
18 experimental protocol. We provide all benchmarking data, results and the entire  
19 benchmarking workflow named QuasiModo, **Quasispecies Metric determination on**  
20 **omics**, under the GNU General Public License v3.0 (<https://github.com/hzibifo/Quasimodo>), to enable full reproducibility and further benchmarking on these and  
22 other data.

## 1 Introduction

2 Human cytomegalovirus (HCMV) causes a lifelong infection that is typically without  
3 major clinical symptoms. After primary infection HCMV persists latently in infected  
4 cells [1]. Primary or (re-)infections and reactivation of HCMV can cause significant  
5 morbidity and severe complications in immunocompromised individuals, such as HIV-  
6 infected persons, transplant recipients or congenitally infected children [2,3]. HCMV  
7 has a double-stranded DNA genome of approximately 235 kb, including terminal and  
8 internal repeats, which contains at least 170 open reading frames [4]. With genome  
9 sizes of known viruses ranging from ~1 kb (*Circovirus SFBeef*) to 2 Mb (*Pandoravirus*  
10 *salinus*) [5], HCMV belongs to the larger known viruses and has co-evolved with its  
11 host for millions of years [6]. Multiple HCMV strain infections (i.e. with more than one  
12 strain at the same time) probably contribute to prolonged viremia, delayed viral  
13 clearance and other complications [7–10].

14 The establishment of high-throughput sequencing techniques and accompanying  
15 bioinformatics analysis methods has greatly advanced viral genomic research [11–16].  
16 Assembling viral genomes of individual virus strains from a mixed population and  
17 variant calling are essential for characterizing the evolution and genetic diversity of  
18 viral pathogens such as HCMV *in vivo*. Although HCMV mutates and evolves more  
19 slowly than many RNA viruses and not any faster than other herpes viruses, high  
20 levels of genetic variation due to mixed (i.e. multiple) viral strain infections in an  
21 individual are often observed [17–20]. These multiple strain infections likely result from  
22 reactivation of latent strains and/or re-infections [17,21,22].

23 Assemblers leverage short read sequence data by linking sequences using kmer or  
24 read graphs, and, in some cases, variant frequencies, to reconstruct viral haplotypes,  
25 such as the recently developed HaROLD [23], which makes use of longitudinal  
26 sequence data. There are also many variant callers available, including programs for  
27 calling low-frequency variants, such as LoFreq [24], VarScan2 [25], and the  
28 commercial CLC Genomics Workbench [26]. Those programs use information on  
29 basecall and mapping quality to determine if a variant site in a read may be due to  
30 sequencing error, mapping bias or reflects true biological diversity [24–26].

31 A recent study on simulated and mock viromes suggests that the choice of assembler  
32 largely influences virome characterization [27]. Several assemblers that we evaluated,

1 including IDBA-UD [28], SPAdes [29], Ray [30] and Megahit [31], were previously  
2 assessed on more divergent, simulated and spiked mock viromes [27,32]. This in one  
3 case included strains of less than 97% average nucleotide identity (ANI) [33], which  
4 resulted in shorter assemblies for low divergent community members. Viral haplotype  
5 assemblers reconstruct small viral genomes, such as HIV, Zika and hepatitis C virus,  
6 with good genome fractions. However, these may be highly fragmented, in case of  
7 Savage [34], or consist of longer contigs with a substantial amount of misassemblies,  
8 in case of PEhaplo [35], QuasiRecomb [36] and PredictHaplotype [37]. Viral haplotype  
9 assemblers have so far been mostly evaluated on much smaller and more divergent  
10 genomes (genome size around 10 kb with divergence of up to 12.7%) [34,38]. They  
11 have not been assessed on substantially larger genomes with low density of variants  
12 so far. A recent assessment of variant callers [39] reported variable, in part  
13 complementary performances of FreeBayes [40], LoFreq, VarDict [41], and VarScan2  
14 in minority variant detection on simulated short read data from Respiratory Syncytial  
15 Virus (RSV), which is a small virus with a 15 kb genome size.

16 So far, strain-level assembly and variant calling methods have not been evaluated for  
17 large DNA viruses, where runtime and memory consumption of the algorithms might  
18 also be critical, nor on benchmark data that include experimental biases of library  
19 preparation and sequencing. To investigate these issues, in the largest benchmark of  
20 its kind so far, we created and sequenced ten samples of HCMV strains with different  
21 mixing ratios and then evaluated 21 computational methods on the resulting WGS  
22 data. Analysis of these lab-created benchmark data sets allowed us to dissect the  
23 effects of computational methods and library preparation protocols.

24

## 25 Results

### 26 Creation and quality control of viral sequence samples

27 To produce a benchmark dataset of mixed viral strains that also includes technical  
28 artifacts introduced in experimental data generation, we created viral strain mixtures  
29 mimicking clinical samples from patients with mixed strain infections *in vitro*. For this,  
30 we combined viral DNA of the HCMV strains TB40/E BAC4 and AD169 (designated  
31 as "TA"), derived directly from bacterial artificial chromosomes (BAC) with these viral

1 genomes and prepared from *Escherichia coli*, or the strains TB40/E BAC4 and Merlin  
2 (designated as “TM”), which were amplified in human cell-cultures, respectively, at  
3 mixing ratios of 1:1, 1:10 and 1:50. The ANIs between each pair of those strains are  
4 around 0.977 (Table S1). In addition, pure strains were sequenced separately in each  
5 experiment, resulting in four data sets with the TB40/E and AD169 strains without  
6 target enrichment and the TB40/E and Merlin strain after enrichment. For the TA  
7 mixture experiments, we used a library preparation protocol (protocol 1, details in  
8 Material and Methods) without target enrichment, for the TM mixtures a protocol  
9 including target enrichment (protocol 2). All ten samples (6 HCMV strain mixtures and  
10 4 pure strains) were sequenced using 2x 300 bp paired-end sequencing (Illumina  
11 MiSeq), resulting in 1.58 million raw reads on average per sample. After quality control,  
12 1.1 million quality reads per sample with average base quality above 30 remained.  
13 As the HCMV strains for the TA mixtures and corresponding pure strain samples were  
14 extracted from *E. coli* BACs, *E. coli* reads were found in those samples with an  
15 average fraction of  $48.6 \pm 16.5\%$  (Table S2). Based on the genome size of HCMV  
16 (235K) and *E. coli* (4.6M), the abundance of contaminating *E. coli* is thus around 5%.  
17 The three TM data sets and the pure Merlin strain, TM-0-1, did not include detectable  
18 bacterial contamination, but 51.7% of the reads of TM-1-0 (pure TB40/E strain) were  
19 of human origin.

20

## 21 Strain-resolved genome assembly

22 For mixed strain data sets, the ultimate aim for assembly is to recover the genomes of  
23 individual strains. To obtain a comprehensive performance overview for existing  
24 software, we evaluated the performances of the generic (meta-)genome assemblers  
25 SPAdes, metaSPAdes [42], Megahit, ABySS [43], Ray, IDBA-UD, Tadpole, which is a  
26 part of the BBMAP toolkit [44] and IVA [45], Vicuna [46], as well as the viral haplotype  
27 assemblers Savage, PredictHaplo, PEhaplo, QuasiRecomb, ShoRAH [47] and  
28 VirGenA [48] on our data sets (Material and Methods).

29 Assemblies were assessed based on common assembly quality metrics with  
30 metaQUAST [49], such as genome fraction, duplication ratio, largest alignment,  
31 NGA50 using both strain genomes as references for the respective mixtures (Methods,  
32 Figure 1). The genome fraction is defined as the fraction of the reference genome

1 covered by at least one contig. The duplication ratio is the number of bases of the  
2 reference genome covered, divided by the total number of aligned bases from the  
3 assembly. The largest alignment is the size of the biggest contig that aligned to the  
4 reference genome. The NGA50 value of an assembly is calculated by first sorting the  
5 aligned contigs, after being split at misassembly events, by size in descending order  
6 and returning the length of the contig that exceeds 50% genome fraction. If an  
7 assembler fails to produce 50% genome fraction, the NGA50 value cannot be  
8 calculated and was set to 0 kb. To further summarize the performance of assemblers  
9 on the HCMV datasets, we defined a composite quality metric for strain-resolved  
10 assembly performances, consisting of a weighted score combining the metaQUAST  
11 assembly metrics “duplication ratio”, “genome fraction”, “largest alignment”, “NGA50”,  
12 “number of contigs”, and “number of mismatches per 100 kb” (Materials and Methods).  
13 In this weighted score, we considered genome fraction and largest alignment the most  
14 important metrics, since they reflect the ability of the assembler to reconstruct  
15 individual strains and the completeness of the largest assembly.

16 All programs reconstructed the genome sequence much better for the dominant than  
17 for the minor strain. With the weighted summary score, metaSPAdes achieved the  
18 highest score (8.57), with a large genome fraction assembled ( $54.5\pm6.4\%$  versus  
19  $45.3\pm12.4\%$  for IVA, mean  $\pm$  standard deviation) and second best for largest alignment  
20 ( $145.9\pm56.6$  kb), NGA50 ( $102.3\pm69.0$  kb), number of contigs ( $12.5\pm9.0$ ) and  
21 duplication ratio ( $1.01\pm0.01$ ) (Figure 1, Table S3-4). Next were IVA (8.12), which was  
22 ranked best for largest alignment, NGA50, and number of contigs, and ABySS (7.50)  
23 (Figure 1, Table S3-4). IVA produced on average the fewest ( $8.1\pm7.9$ ), and longest  
24 contigs ( $159.6\pm77.8$  kb), especially for abundant strains ( $160.8\pm72.3$  kb) (1/0, 50/1,  
25 10/1), with only very few parts of the genomes covered multiple times (duplication ratio  
26 of  $1.01\pm0.03$ ) (Figure 1-2, Table S3). The Tadpole assembly had the lowest duplication  
27 ratio ( $1.001\pm0.001$ ) and the fewest mismatches per 100 kb ( $32.2\pm54.4$ , Figure 1-2,  
28 Table S3). However, this was mainly because it assembled very little data and  
29 generated short contigs (NGA50  $10.9\pm15.4$  kb) that covered less than half  
30 ( $33.8\pm15.6\%$ ) of the underlying genomes.

31 The haplotype assembler Savage in reference-based mode recovered the most  
32 ( $64.4\pm27.2\%$  genome fraction) of both strains, even for the low abundant ones (1/10,  
33 1/50) (Figure 2). However, it produced shorter contigs (largest contig length  $21.5\pm22.8$

1 kb) and many duplicates ( $1.38 \pm 0.23$ ). Megahit recovered most ( $93.4 \pm 5.7\%$ ) of the  
2 genome sequence for the dominant strains, followed by ABySS ( $92.7 \pm 3.1\%$ ), SPAdes  
3 ( $91.8 \pm 4.1\%$ ) and Ray ( $91.6 \pm 7.8\%$ ), however much less for the low abundant strains  
4 ( $38.3 \pm 20.0\%$ ,  $37.3 \pm 14.5\%$ ,  $35.2 \pm 6.6\%$ ,  $12.2 \pm 4.5\%$ , respectively). MetaSPAdes and  
5 IVA also recovered a relatively large fraction ( $83.4 \pm 28.2\%$  and  $86.4 \pm 21.2\%$ ,  
6 respectively) of the dominant strains, but only little ( $38.7 \pm 28.4\%$  and  $8.5 \pm 6.0\%$   
7 respectively) of the genome for low abundant strains.

8 All other haplotype assemblers, *i.e.* Savage in *de novo* mode, PredictHaplo, PEhaplo,  
9 QuasiRecomb, ShoRAH and VirGenA, assembled no contigs and were terminated  
10 after running for more than 10 days using 24 CPU cores. Furthermore, we also tested  
11 1000 random weights sets to calculate the summary score, and the top two  
12 assemblers (metaSPAdes and IVA) maintained this ranking for  $\sim 850$  out of 1000 sets.  
13 This suggests that the assemblers with good performance deliver a high quality  
14 assembly across most metrics.

15 As genome assembly can be computationally intensive and time consuming, we also  
16 benchmarked the disk space consumption (IO output), memory (maximum memory  
17 requirement) and run time of the different algorithms. Ray and ABySS used less than  
18 300 MB for the output while IVA, SPAdes, metaSPAdes and Savage consumed more  
19 than 20 GB of disk space for output or intermediate output (Figure 3). Megahit was the  
20 most memory efficient assembler, using less than 1 GB memory, whereas ABySS,  
21 Savage and Vicuna consumed more than 10 GB. As to the run times, Megahit required  
22 around ten minutes for each assembly, while Vicuna and Savage needed more than  
23 20 hours on a server with sixty-two 2.4GHZ CPUs, 200 TB disk space and 1 TB  
24 memory.

25

## 26 Variant calling

27 We evaluated the variant callers LoFreq, VarScan2, the low frequency variant caller  
28 of the CLC genomics workbench, BCFtools [50], FreeBayes and the GATK  
29 HaplotypeCaller [51] on the six mixed strain and four pure strain (three different strains,  
30 details in material and methods) WGS samples. A ground truth was generated by  
31 pairwise genome alignment of the respective strains with MUMmer [52] (Methods,

1 Figure 4), which identified around 3500-4000 variants, including ~200 short insertions  
2 and deletions (InDels). Sites in these genomes were then classified as variant or non-  
3 variant in this alignment, and compared to predicted variants, to determine true  
4 positive (TP), false negative (FN) and false positive (FP) calls. Since the major strain  
5 in each mixture was used as reference, we could evaluate the performance of those  
6 variant callers in identifying low frequency variants originating from the minor strain in  
7 the mixture, with the expected low frequency variants being 2% and 10%, respectively,  
8 in the mixtures with ratios of 1:50 and 1:10. Variant calls for which a false nucleotide  
9 was predicted for a variant site were also considered as false positives. Based on the  
10 number of TP, FN and FPs we calculated precision, recall and the F1-score as  
11 detection quality metrics for each caller and sample. Precision, or purity, reflects the  
12 fraction of predicted variants that are true variants:  $precision = \frac{TP}{TP+FP}$ ; it thus quantifies  
13 how reliable the predictions of a particular method are. Recall is sometimes also  
14 known as completeness, and measures the fraction of truly existing variants in a data  
15 set that have been detected by a caller ( $recall = \frac{TP}{TP+FN}$ ), it thus measures how  
16 complete the predictions of a caller are with respect to the variants that are there to  
17 discover. To allow a comparison based on a single metric, the F1-score is commonly  
18 used, which is the harmonic mean of precision and recall, i.e.  $F_1 = 2 \times \frac{precision \times recall}{precision + recall}$ .

19 Applying the commonly used cutoff of 20 for Phred quality scores (QUAL) [53] for  
20 accepting predicted variants, we evaluated the performance of variant callers on single  
21 nucleotide polymorphisms (SNPs). LoFreq achieved the best average precision  
22 ( $0.940 \pm 0.011$ ) and VarScan2 the highest recall ( $0.872 \pm 0.050$ , Figure 5A, Table S5)  
23 across mixture samples. LoFreq and VarScan2 consistently performed best across  
24 samples, with average F1-scores, of  $0.890 \pm 0.009$  and  $0.880 \pm 0.011$ , respectively  
25 (Figure 5B, Table S5). CLC had a slightly lower F1-score ( $0.806 \pm 0.025$ ), and was more  
26 variable in performance across samples, while BCFtools, GATK and Freebayes  
27 performed poorly (F1-score:  $0.166 \pm 0.288$ ,  $0.261 \pm 0.388$  and  $0.289 \pm 0.428$ ,  
28 respectively), particularly due to low recall ( $0.122 \pm 0.230$ ,  $0.215 \pm 0.338$  and  
29  $0.253 \pm 0.386$ ). Across all strains and abundance ratios tested, LoFreq consistently  
30 performed well, while VarScan2 was consistent across abundance ratios but  
31 performed differently for the two strain mixtures (varied in precision) and CLC's recall  
32 dropped dramatically for mixture TM-1-50. BCFtools, GATK and FreeBayes performed

1 poorly in comparison for all samples, and for highly diluted samples, their recall was  
2 almost 0. To analyze the effect of their returned Phred quality scores on variant callers'  
3 performances, we evaluated both SNPs and InDels called with different thresholds for  
4 their quality scores using a recall-precision curve. LoFreq had the best recall-precision  
5 balance followed by VarScan2 and CLC, while FreeBayes demonstrated high  
6 performance on samples TA-1-1 and TM-1-1 (Figure S1). To compare variant caller  
7 performances under optimized performance conditions, we also determined  
8 performances of variants called using the best F1-scores over these different settings  
9 across all samples. Notably, the performance of FreeBayes increased substantially,  
10 and that of CLC slightly, while the performances of other methods remained similar  
11 (Figure 5C and 5D, Figure S2, Table S6).

12 The callers achieving good recall, LoFreq, CLC and VarScan2, identified around 2400  
13 to 2700 shared true positive SNPs from all mixed strain samples when using a quality  
14 score threshold of 20 (Figure 6). On the pure strain samples, where no SNPs were  
15 expected, LoFreq and VarScan2 predicted  $61\pm33$  and  $71\pm42$  false positives,  
16 respectively, substantially less than for the mixed strain samples ( $164\pm59$  and  
17  $381\pm163$ ). Notably, of these false positives in mixtures,  $70.7\pm17.3\%$  (based on LoFreq  
18 predictions) and  $37.6\pm7.9\%$  (based on VarScan2) were shared (Figure S3). This  
19 significant overlap (Fisher's exact test p-value  $<2.2\times10^{-16}$ , odds ratio  $3416.8\pm1601.1$ ),  
20 indicates a systematic shared bias regardless of variant callers. Variant calling (Figure  
21 S4) indicated that allele frequencies intended by dilutions were closely reached with  
22 protocol 2 (TM mixture) and differed slightly more for protocol 1 (TA mixture).

23

## 24 Genomic context of variant calls

25 We analyzed whether there was a specific genomic signal associated with variant calls,  
26 considering separately correct and false calls using mutational context analysis [54–  
27 56]. Focusing exemplarily on LoFreq, this approach analyzes the frequency of a  
28 certain SNP together with its sequence context, specifically the flanking 3' and 5' bases.  
29 For the predictions of a certain caller, the genomic context of the six substitution types  
30 (C to A, C to G, C to T, T to A, T to C and T to G) was calculated with the R package  
31 SomaticSignatures [56] for the six mixtures and four pure strain samples (2 samples  
32 of TB40/E, 1 of Merlin, and 1 of AD169). Since the analysis is not strand-specific, the

1 above were considered equivalent with G to T, G to C, G to A, A to T, A to G and A to  
2 C, respectively. We observed a strong, context-independent preference for C to T or  
3 T to C transitions (with a fraction of  $0.803 \pm 0.016$  of all variant calls across samples;  
4 top panel of Figure 7A and Figure 7B), which was even more pronounced for the true  
5 positives (middle panel of Figure 7A and Figure 7B), but not for FPs. For variants  
6 observed across pairwise combinations of 30 *E. coli* and 30 HIV genomes, which were  
7 obtained from NCBI RefSeq database (Table S7), respectively, we observed  
8 concordant results (Figure S5-S6). For these data, transitions accounted for  
9  $0.716 \pm 0.058$  and  $0.681 \pm 0.017$  of variants between genome pairs, respectively.

10 We found a pronounced context dependent signal for false positive calls of LoFreq  
11 and VarScan2. Here, T to G variants in a G.G context correspond mostly to FPs in the  
12 TA and TM mixtures ( $57.1 \pm 10.0\%$  and  $86.8 \pm 18.3\%$ , respectively; bottom panel of  
13 Figure 7A and Figure 7B). This enrichment is highly significant (p-value  $<0.0001$ ,  
14 Fisher's exact test), with an odds ratio of around 45.2 for the TM mixture; i.e. T to G  
15 calls are 45.2 times more frequent in this context than in others and 19.9 more frequent  
16 for the TA mixture. For false variant calls on the pure Merlin and AD169 samples, T to  
17 G calls in a G.G context were even more dominant. For LoFreq on the pure Merlin  
18 (TM-0-1) sample, the genomic context pattern of false calls is highly correlated with  
19 the context pattern of false positives for all mixed strain samples, with an average  
20 Pearson correlation of 0.903 (p-value  $<0.0001$ ). For the AD169 strain and respective  
21 mixtures, this correlation (Pearson) is lower, on average 0.697, but still highly  
22 significant (p-value  $<0.0001$ ).

23 The allele frequencies of the FP LoFreq variants were substantially lower than those  
24 of the true positive variants (Figure S7, Wilcoxon test p-value  $<2.2 \times 10^{-16}$ ), except for  
25 the TA-1-50 sample, which had the highest-level *E. coli* cloning vector contamination.  
26 False T to G calls in a G.G context had a lower frequency than other false calls (p-  
27 value  $1.181 \times 10^{-10}$  for TM mixtures: Figure S8,  $8.16 \times 10^{-10}$  for TA mixtures). The allele  
28 frequency of those FP SNPs was slightly lower in protocol 2 (TM,  $0.0237 \pm 0.0522$ ) than  
29 in protocol 1 (TA,  $0.0242 \pm 0.0121$ ) with a Wilcoxon p-value = 0.000559, 95% CI =  
30  $[0.00363, 0.0120]$ . The extent of the signal differed between samples created with  
31 different protocols. Though the overall FP rate was similar, the context-dependent  
32 false calls T to G in G.G doubled in protocol 2 (Figure 7A, 7B). We found no such  
33 signal for false LoFreq variants calls on MiSeq sequencing data from HIV lab data [57],

1 even though the frequency of GTG/CAC patterns in both genomes are similar (Figure  
2 S9).

3

4 **Materials and methods**

5 **Creation and sequencing of HCMV strain mixtures**

6 We created mixtures for two pairs of strains: “TB40/E BAC4” with “AD169 subclone  
7 HB5” (TA) and TB40/E BAC4 with strain Merlin (TM). For each strain pair, mixtures  
8 with three different mixing ratios, 1:1, 1:10 and 1:50, were created. Accordingly, strains  
9 “AD169” and “Merlin” are the dominant strains in the mixtures, and their genomes were  
10 used as reference for variant calling in mixed samples. In addition, the pure strains  
11 were sequenced. The name of the mixture specifies the included strains and the  
12 mixing ratio. For instance, a mixture of TB40/E and Merlin with a ratio of 1:10 is  
13 denoted by TM-1-10. Pure strain samples are denoted as TA-1-0 for TB40/E and TA-  
14 0-1 for AD169, which were created with protocol 1 (details, see below), as well as TM-  
15 1-0 for TB40/E and TM-0-1 for Merlin, created with protocol 2.

16 Two protocols were used to generate the sequencing libraries. In protocol 1, the DNA  
17 of TA mixtures (TA-1-1, TA-1-10 and TA-1-50) and pure strain samples (TA-0-1, TA-  
18 1-0) was extracted from the BAC host *E. coli* strain GS1783 using the Plasmid Midi Kit  
19 (Macherey Nagel). Library preparation was performed using an Ultra II FS-Kit from  
20 NEB according to the standard protocol from the manufacturer. Fragmentation time  
21 was 10 minutes and the library was amplified 4 cycles for the mixtures and 5 cycles  
22 for the pure BACs, multiplexed and sequenced on a MiSeq (Illumina) using reagent kit  
23 v3 to generate 2 × 300 bp paired-end reads.

24 Protocol 2 was used to generate the TM mixture data sets (TM-1-1, TM-1-10, TM-1-  
25 50) and the pure strain samples data sets (Merlin, TM-0-1 and TB40/E BAC4, TM-1-  
26 0). The HCMV strains TB40/E BAC4 and Merlin were isolated from cell cultures. The  
27 library preparation was performed as we previously described [20] with the KAPA  
28 library preparation kit (KAPA Biosystems, USA) with a few modifications. After PCR  
29 pre-amplification (6-14 cycles) with adapter specific primers, up to 750 ng of DNA was  
30 target enriched for HCMV fragments using HCMV specific RNA baits. HCMV enriched  
31 libraries were indexed, amplified (17 to 20 cycles) using TruGrade oligonucleotides

1 (Integrated DNA Technologies), multiplexed and sequenced on a MiSeq (Illumina)  
2 using reagent kit v3 to generate 2 × 300 bp paired-end reads.

3

4 **Quality control of the sequencing data**

5 Sequencing reads produced by the MiSeq sequencer were quality controlled using  
6 fastp v0.19.4 [58]. Fastp is an all in one FASTQ data preprocessing toolkit with  
7 functionalities including quality control, adapter detection, trimming, error correction,  
8 sequence filtering and splitting. The remaining adapter sequences were clipped from  
9 the raw reads as well as bases at the 5' or 3' of the reads with a base quality score of  
10 less than 20. Reads shorter than 130 bp after trimming were removed. The remaining  
11 PhiX sequences (originating from the Illumina PhiX spike-in control) were also  
12 removed from the dataset by mapping all quality-controlled reads against the PhiX  
13 reference genome downloaded from Illumina using BWA-MEM v0.7.17 [59].  
14 Contamination from *E. coli* and the human host were also removed using the same  
15 method.

16

17 **Consensus assembly and evaluation**

18 To benchmark the performance of commonly used assemblers, we evaluated SPAdes  
19 v3.12.0 (with kmer sizes: 21, 33, 55, 77, 99, 127 and --careful option), metaSPAdes  
20 v3.12.0 (kmer sizes: 21, 33, 55, 77, 99, 127), Megahit v1.1.3 (kmer sizes: 21, 41, 61,  
21 81, 101, 121, 141, 151, ), Ray (kmer size: 31), ABySS v2.1.4 (kmer size: 96), IDBA  
22 v1.1.3 (default settings), Tadpole v37.99 (default settings), IVA v1.0.9 (default settings)  
23 and Vicuna v1.3 (default settings). The quality of the resulting contigs or scaffolds was  
24 then assessed with metaQUAST v5.0.2. Only contigs longer than 500 bp were taken  
25 into account. Since the reference genomes of those strains are highly similar, with an  
26 ANI around 98%, only unique mappings were considered in the assessment, i.e. not  
27 allowing a single contig to map to both reference genomes in the combined reference  
28 report. The metrics include the overall number of aligned contigs, the largest alignment,  
29 genome fraction, duplicate ratio, NGA50, number of mismatches per 100 kb. Here,  
30 “largest alignment” refers to the largest contig or scaffold that mapped to the reference  
31 genome. “Genome fraction” represents the fraction of the genome recovered by

1 contigs from an assembly. The “duplication ratio” is the total number of aligned bases  
2 in the assembly divided by the total number of those in the reference  
3 (<https://github.com/ablab/quast>). NGA50 is the N50 value of the contigs that mapped  
4 to the reference genomes with contigs being split at misassemblies. The NGA50 value  
5 cannot be calculated for the assemblies which recover less than 50% of the genome  
6 in terms of genome fraction and was set to 0 instead to ensure comparability. The  
7 individual reference report from metaQUAST was used to evaluate the performance  
8 for abundant or low abundant strains in mixtures. All overall metrics values regardless  
9 of the specific strain in the mixture were calculated using the combined reference  
10 report from metaQUAST, except for NGA50.

11

## 12 Haplotype reconstruction

13 Of viral quasispecies assemblers, we ran PEHaplo v0.1, PredictHaplo v0.4, Savage  
14 v0.4.0, QuasiRecomb v1.2, ShoRAH v1.9.95 and VirGenA v1.4 using default settings  
15 (for details see the code repository). We did not run HaROLD, as this requires  
16 longitudinal clinical samples from the same source. The haplotype assemblies were  
17 evaluated using metaQUAST together with the consensus assemblies mentioned  
18 above.

19

## 20 A composite quality metric for strain-resolved assembly

21 To summarize assembly performances, we defined a weighted score based on the  
22 metaQUAST assembly metrics using combined reference including genome fraction,  
23 largest alignment, NGA50, duplication ratio, number of contigs, and number of  
24 mismatches per 100 kb. As NGA50 is not available in the combined reference report  
25 of metaQUAST, we used the average NGA50 based on individual genomes from the  
26 individual references report. Of these metrics, we considered genome fraction and  
27 largest alignment as the most important metrics, since they reflect the ability of the  
28 assembler to reconstruct individual strains. To calculate a weighted summary score  
29 for assembler performance, we weighted the above metrics by the factors 0.3, 0.3, 0.1,  
30 0.1, 0.1 and 0.1 (genome fraction, largest alignment, NGA50, duplication ratio, number

1 of contigs, and number of mismatches per 100 kb), respectively. The score of an  
2 assembler with metric  $i$  was formulated based on the scale average performance  $sp_i$   
3 and then multiplied by a factor of 10 to ensure the score is in the range of 0-10:

4 
$$score_i = 10 \times weight_i \times sp_i$$

5 , where  $sp_i$  is the scaled performance for metric  $i$ . The value was scaled into 0-1  
6 with min-max normalization defined as follows:

7 
$$sp_i = \begin{cases} \frac{p_i - min}{max - min}, & \text{if } p \text{ bigger better} \\ \frac{max - p_i}{max - min}, & \text{if } p \text{ smaller better} \end{cases}$$

8 In the formula,  $p_i$  is the average performance across all samples of the given  
9 assembler for metric  $i$  and the min and max are the smallest and largest average  
10 performance value on metric  $i$  among all assemblers.

11

## 12 Determination of genome differences between two strains

13 MUMmer v3.23 with default setting was used to align two genomes of the strains in  
14 each mixture and to identify the differences between genomes as ground  
15 truth. Command “show-snps” of the MUMmer package was employed to determine  
16 the SNPs and short InDels differing between two aligned genomes with parameter  
17 setting “--CTHr”, where the repeat regions were masked. The genomic differences  
18 between TB40/E and Merlin were considered as the ground truth variants for the TM  
19 mixtures, while differences between TB40/E and AD169 were considered as the  
20 ground truth for the TA mixtures.

21

## 22 Variant calling

23 Quality controlled reads were mapped against the reference genome of the HCMV  
24 strains Merlin and AD169 using BWA-MEM with a seed length of 31. HCMV Merlin  
25 and AD169 genomes were used as reference genomes, as they were the major strains  
26 in all mixtures. The resulting BAM files were deduplicated with the Picard package  
27 (<http://broadinstitute.github.io/picard/>) to remove possible amplification duplicates that

1 may bias the allele frequency of identified variants. To compare the performance of  
2 different variant callers, we used LoFreq (parameter: -q 20 -Q 20 -m 20), VarScan2 (-  
3 --min-avg-qual 20 --p-value 0.01), FreeBayes (--p 1 -m 20 -q 20 -F 0.01 --min-  
4 coverage 10), CLC (overall read depth  $\geq$ 10, average basecall quality  $\geq$ 20,  
5 forward/reverse read balance 0.1-0.9 and variant frequency  $\geq$ 0.1%), BCFtools (--p  
6 0.01 --ploidy 1 -mv -Ob) and GATK HaplotypeCaller (--min-base-quality-score 20 -  
7 ploidy 1) to identify variants. The variants from the difference between genomes  
8 detected by MUMmer were considered as positive variants. Based on this standard,  
9 precision, recall, and F1-score were computed to evaluate those callers. The pairwise  
10 genome differences of 30 *E. coli* or 30 HIV genomes were determined by MUMmer as  
11 well. To evaluate the performance of different callers for SNP and InDel prediction, the  
12 command vcfeval in RTG-tools [60] was used to generate recall-precision curves  
13 based on the Phred scaled “QUAL” score field (--squash-ploidy -f QUAL --sample ALT).

14

## 15 Data and code availability

16 The benchmarking program developed in this study is available under the GNU  
17 General Public License V3.0 at <https://github.com/hzi-bifo/Quasimodo>. This program  
18 can be also used to assess variant calling and assembly results for other viral mixed  
19 strain data sets (see readme of the repository for details). All assembly and variant  
20 calling results are freely accessible on Zenodo (10.5281/zenodo.3739874). The  
21 sequence data were deposited in ENA with accession number PRJEB32127.

22

## 23 Discussion and conclusions

24 Mixed infections with multiple HCMV strains are commonly observed in patients with  
25 active HCMV replication [10,17–20]. Accurately reconstructing the genomic  
26 sequences of the individual haplotypes has implications for gaining a deeper  
27 understanding of viral pathogenicity and viral diversity within the host. To identify the  
28 most suitable software for analysis of mixed viral genome sequencing samples with  
29 low evolutionary divergence and comparatively large genomes, we evaluated multiple

1 state-of-the-art assemblers and variant callers on lab-generated strain mixtures of  
2 HCMV.

3 In the assembly benchmarking, most metagenome and genome assemblers, in  
4 particular metaSPAdes and IVA, recovered the abundant strains well in terms of  
5 metrics such as genome fraction, contig length and mismatches. When also  
6 considering strains of low abundance, Savage recovered the largest fractions of both  
7 underlying genomes in the reference-based mode. However, this was achieved in a  
8 highly fragmented manner, consistent with reports by the authors (Table 3 [34]). Thus,  
9 the state-of-the-art in assembly methods, including both generic (meta-)genome and  
10 specialized viral quasispecies assemblers, does not yet reconstruct large viral HCMV  
11 genomes of low abundance and low variant density with high quality. This may not be  
12 surprising since these programs were originally designed primarily for mixtures of  
13 large and much more divergent microbial genomes, or for viral genomes with a tenth  
14 of the size of the HCMV genome, but a higher variant density. In terms of resource  
15 usage, Ray and ABySS produced the smallest outputs, while megahit was the most  
16 memory efficient, as well as fastest assembler with good performance (weighted  
17 score >5).

18 Of the variant callers, LoFreq most faithfully identified only true variants across all  
19 samples, closely followed by VarScan2. Both had high F1-scores even on the samples  
20 with high mixing ratios. When analyzing the genomic context of the predicted variants,  
21 for true positive calls, we observed a context independent enrichment of T to C and C  
22 to T transitions. A preference for transitions over transversions is common in molecular  
23 evolution [61,62]. This is the case in terms of observed mutations and because  
24 transitions more often lead to synonymous mutations that tend to be neutral, rather  
25 than under negative selection, as most nonsynonymous changes on the population  
26 level.

27 For false variant calls, we found a striking enrichment of T to G changes in a G.G  
28 context, representing an unreported context-dependent signal. Calls with this pattern  
29 had lower allele frequencies than true positive variant calls and were more pronounced  
30 in sample with more PCR cycles used (protocol 2, 6-14 cycles versus 4 in protocol 1),  
31 indicating a link to DNA amplification. Amplification error introduced in PCR cycles will  
32 accumulate exponentially and occur at frequencies that depend on when they were  
33 introduced: PCR-induced errors are mostly of lower frequency unless introduced in

1 one of the very early amplification cycles [57]. Schirmer and co-workers studied the  
2 error profiles for the amplicon sequencing using MiSeq with different library  
3 preparation methods and showed that the library preparation method and the choice  
4 of primers are the most significant sources of bias and cause distinct error patterns  
5 [63]. They also observed a run-specific preference for the substituting nucleotide. They  
6 observed that A and C were more prone to substitution errors (A to C and C to A)  
7 compared to G and T, which differ from our results. We could not find the context  
8 dependent signal for an HIV quasispecies data set that had been generated with  
9 Nextera XT DNA Library Prep chemistry (Illumina) on Illumina's MiSeq platform,  
10 suggesting that the false positive pattern originates from a step unique to the HCMV  
11 sequencing protocol, such as pre-amplification and amplification PCR during library  
12 preparation.

13 Notably, the experimental protocols substantially affected the nature of the generated  
14 data and bioinformatics results. Protocol 1 led to substantial amplification of *E. coli*  
15 host DNA and thus lower coverage of the viral strains. This, together with the resulting  
16 differences in actual mixing ratios relative to protocol 2 likely explain the higher recall  
17 and slightly lower precision observed in variant detection (Figure S4). An earlier study  
18 based on simulated sequencing data also showed that variant calling on lower  
19 coverage samples achieved higher recall and lower precision [64]. Protocol 2 used  
20 more extensive DNA amplification together with cultivation in human cell culture. This  
21 resulted in higher coverage of viral strain genomes in comparison to protocol 1, and  
22 the doubling of context-dependent false positive variant calls within a G.G context  
23 discussed above (Figure 7).

24 Taken together, our results suggest that for strain mixtures of large DNA viruses with  
25 low variant density, many assemblers reconstruct the abundant strain with high quality,  
26 but assembly of the low abundant strains is still challenging. Variant callers designed  
27 for low frequency variant detection provided the best results and detected most true  
28 variants. These findings are relevant for the interpretation of program outputs when  
29 analyzing clinical patient samples. We also provide a resource that facilitates further  
30 benchmarking, including our result evaluation and visualization software QuasiModo,  
31 all produced benchmarking data sets and results, for flexible assessment of further  
32 methods on these and similar data sets.

1

## 2 Key points

- 3 • The strain-resolved *de novo* assembly of large DNA virus with low variant  
4 density is challenging to all evaluated assemblers. Some generic  
5 (meta-)genome assemblers, such as metaSPAdes and IVA, performed  
6 particularly well in recovering the dominant strain.
- 7 • LoFreq and VarScan2 are good choices for identifying low frequency variants  
8 from strain mixture of large DNA viruses.
- 9 • The pattern of false variant calls likely links to the experimental protocol used  
10 to generate the sequencing data. More amplification cycles led to more  
11 pronounced false positive variant calls.
- 12 • All the analyses can be reproduced using QuasiModo developed in this study.  
13 QuasiModo can be also utilized to evaluate other methods using the  
14 benchmarking data sets in this study or similar data sets.

15

## 16 Acknowledgments

17 We thank Dr. Till-Robin Lesker and Susanne Reimering for helpful comments. This  
18 work is supported by German Center for Infection Research (DZIF), Hannover-  
19 Braunschweig site, TI Bioinformatics Platform and TTU Infections of the  
20 Immunocompromised Host, as well as by the Deutsche Forschungsgemeinschaft  
21 through the Collaborative Research Center 900 “Chronic Infections”. A. Dhingra and  
22 J. Götting were supported by the graduate program “Infection Biology” of the Hannover  
23 Biomedical Research School.

24

## 1 **Description of the authors**

2 **Z.-L. Deng** is a post-doctoral researcher at the Department Computational Biology of  
3 Infection Research of the Helmholtz Centre for Infection Research. His research  
4 focuses on viral genomics and microbiome.

5 **A. Dhingra** was a PhD student at the Institute of Virology in Hannover Medical  
6 School working on next generation sequencing of viruses. He is currently a post-  
7 doctoral researcher.

8 **A. Fritz** is a PhD student at the Department Computational Biology of Infection  
9 Research of the Helmholtz Centre for Infection Research. He focuses on developing  
10 software for strain-resolved assembly and metagenomics.

11 **J. Götting** is a PhD student at the Institute of Virology in Hannover Medical School  
12 working on next generation sequencing of viruses and NGS data analysis.

13 **P. C. Münch** is a PhD student at the Department Computational Biology of Infection  
14 Research of the Helmholtz Centre for Infection Research and Max von Pettenkofer  
15 Institute in Ludwig Maximilian University of Munich.

16 **L. Steinbrück** is working on next generation sequencing at the Institute of Virology  
17 in Hannover Medical School.

18 **T. F. Schulz** is the director of Institute of Virology in Hannover Medical School. And  
19 his research focuses on virology and infection.

20  
21 **T. Ganzenmüller** was working as a clinical virologist at the Institute of Virology in  
22 Hannover Medical School. She is currently working at the Institute for Medical  
23 Virology in University Hospital Tübingen as a senior physician.

24  
25 **A. C. McHardy** is the head of Department Computational Biology of Infection  
26 Research of the Helmholtz Centre for Infection Research. The department studies  
27 the human microbiome, viral and bacterial pathogens, and human cell lineages  
28 within individual patients by analysis of large-scale biological and epidemiological  
29 data sets with computational techniques.

30

## 1    References

## 2

3    1. Goodrum F, Caviness K, Zagallo P. Human cytomegalovirus persistence. *Cell. Microbiol.*  
4    2012; 14:644–655

5    2. Griffiths P, Baraniak I, Reeves M. The pathogenesis of human cytomegalovirus. *J. Pathol.*  
6    2015; 235:288–297

7    3. Manicklal S, Emery VC, Lazzarotto T, et al. The ‘silent’ global burden of congenital  
8    cytomegalovirus. *Clin. Microbiol. Rev.* 2013; 26:86–102

9    4. Dolan A, Cunningham C, Hector RD, et al. Genetic content of wild-type human  
10   cytomegalovirus. *J. Gen. Virol.* 2004; 85:1301–1312

11   5. Campillo-Balderas JA, Lazcano A, Becerra A. Viral Genome Size Distribution Does not  
12   Correlate with the Antiquity of the Host Lineages. *Front. Ecol. Evol.* 2015; 3:728

13   6. Murthy S, O’Brien K, Agbor A, et al. Cytomegalovirus distribution and evolution in  
14   hominines. *Virus Evol* 2019; 5:vez015

15   7. Nichols WG, Corey L, Gooley T, et al. High risk of death due to bacterial and fungal  
16   infection among cytomegalovirus (CMV)-seronegative recipients of stem cell transplants  
17   from seropositive donors: evidence for indirect effects of primary CMV infection. *J. Infect.*  
18   *Dis.* 2002; 185:273–282

19   8. Manuel O, Asberg A, Pang X, et al. Impact of genetic polymorphisms in cytomegalovirus  
20   glycoprotein B on outcomes in solid-organ transplant recipients with cytomegalovirus  
21   disease. *Clin. Infect. Dis.* 2009; 49:1160–1166

22   9. Vinuesa V, Bracho MA, Albert E, et al. The impact of virus population diversity on the  
23   dynamics of cytomegalovirus DNAemia in allogeneic stem cell transplant recipients. *J. Gen.*  
24   *Virol.* 2017; 98:2530–2542

25   10. Arav-Boger R. Strain Variation and Disease Severity in Congenital Cytomegalovirus  
26   Infection: In Search of a Viral Marker. *Infect. Dis. Clin. North Am.* 2015; 29:401–414

27   11. Datta S, Budhaujiya R, Das B, et al. Next-generation sequencing in clinical virology:  
28   Discovery of new viruses. *World J Virol* 2015; 4:265–276

29   12. Liu S, Chen Y, Bonning BC. RNA virus discovery in insects. *Current Opinion in Insect*  
30   *Science* 2015; 8:54–61

31   13. Quick J, Loman NJ, Duraffour S, et al. Real-time, portable genome sequencing for Ebola  
32   surveillance. *Nature* 2016; 530:228–232

33   14. Quick J, Grubaugh ND, Pullan ST, et al. Multiplex PCR method for MinION and Illumina  
34   sequencing of Zika and other virus genomes directly from clinical samples. *Nat. Protoc.*  
35   2017; 12:1261–1276

36   15. Ali R, Blackburn RM, Kozlakidis Z. Next-Generation Sequencing and Influenza Virus: A  
37   Short Review of the Published Implementation Attempts. *HAYATI Journal of Biosciences*  
38   2016; 23:155–159

39   16. Martí-Carreras J, Maes P. Human cytomegalovirus genomics and transcriptomics  
40   through the lens of next-generation sequencing: revision and future challenges. *Virus Genes*  
41   2019; 55:138–164

42   17. Cudini J, Roy S, Houldcroft CJ, et al. Human cytomegalovirus haplotype reconstruction  
43   reveals high diversity due to superinfection and evidence of within-host recombination. *Proc.*  
44   *Natl. Acad. Sci. U. S. A.* 2019; 116:5693–5698

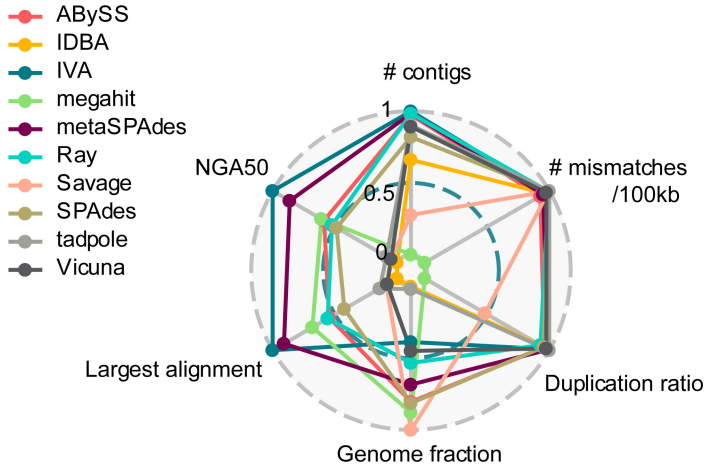
45   18. Suárez NM, Wilkie GS, Hage E, et al. Human Cytomegalovirus Genomes Sequenced  
46   Directly From Clinical Material: Variation, Multiple-Strain Infection, Recombination, and Gene  
47   Loss. *J. Infect. Dis.* 2019; 220:781–791

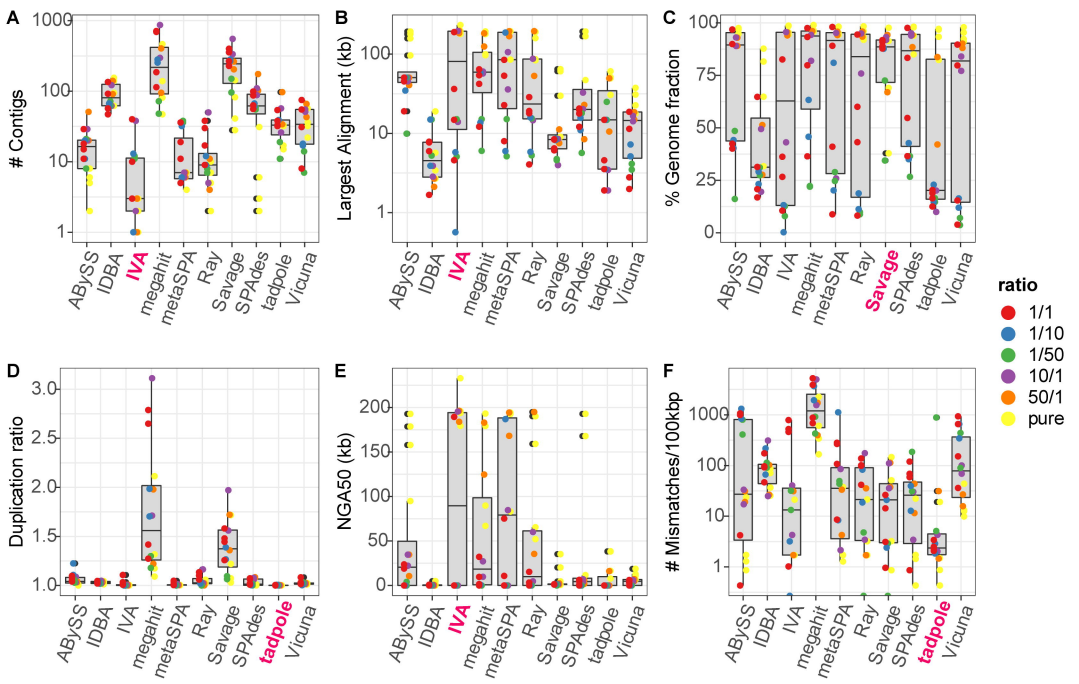
48   19. Suárez NM, Musonda KG, Escrivá E, et al. Multiple-Strain Infections of Human  
49   Cytomegalovirus With High Genomic Diversity Are Common in Breast Milk From Human  
50   Immunodeficiency Virus-Infected Women in Zambia. *J. Infect. Dis.* 2019; 220:792–801

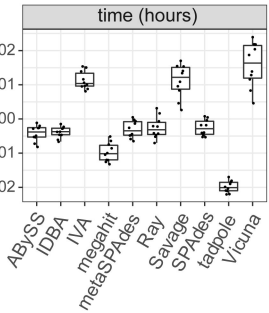
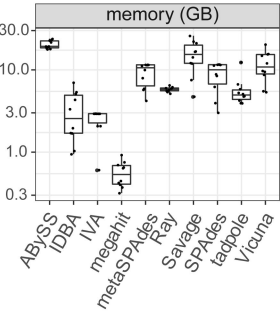
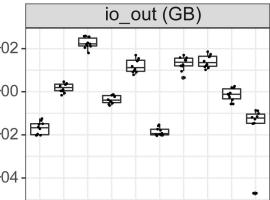
51   20. Hage E, Wilkie GS, Linnenweber-Held S, et al. Characterization of Human  
52   Cytomegalovirus Genome Diversity in Immunocompromised Hosts by Whole-Genome  
53   Sequencing Directly From Clinical Specimens. *J. Infect. Dis.* 2017; 215:1673–1683

- 1 21. Chou SW. Acquisition of donor strains of cytomegalovirus by renal-transplant recipients.
- 2 N. Engl. J. Med. 1986; 314:1418–1423
- 3 22. Puchhammer-Stöckl E, Görzer I, Zoufaly A, et al. Emergence of multiple
- 4 cytomegalovirus strains in blood and lung of lung transplant recipients. Transplantation
- 5 2006; 81:187–194
- 6 23. Goldstein RA, Tamuri AU, Roy S, et al. Haplotype assignment of virus NGS data using
- 7 co-variation of variant frequencies. bioRxiv 2018; 444877
- 8 24. Wilm A, Aw PPK, Bertrand D, et al. LoFreq: a sequence-quality aware, ultra-sensitive
- 9 variant caller for uncovering cell-population heterogeneity from high-throughput sequencing
- 10 datasets. Nucleic Acids Res. 2012; 40:11189–11201
- 11 25. Koboldt DC, Zhang Q, Larson DE, et al. VarScan 2: somatic mutation and copy number
- 12 alteration discovery in cancer by exome sequencing. Genome Res. 2012; 22:568–576
- 13 26. . CLC Manuals - [clcsupport.com](http://clcsupport.com).
- 14 27. Sutton TDS, Clooney AG, Ryan FJ, et al. Choice of assembly software has a critical
- 15 impact on virome characterisation. Microbiome 2019; 7:12
- 16 28. Peng Y, Leung HCM, Yiu SM, et al. IDBA-UD: a de novo assembler for single-cell and
- 17 metagenomic sequencing data with highly uneven depth. Bioinformatics 2012; 28:1420–
- 18 1428
- 19 29. Bankevich A, Nurk S, Antipov D, et al. SPAdes: a new genome assembly algorithm and
- 20 its applications to single-cell sequencing. J. Comput. Biol. 2012; 19:455–477
- 21 30. Boisvert S, Raymond F, Godzariadis E, et al. Ray Meta: scalable de novo metagenome
- 22 assembly and profiling. Genome Biol. 2012; 13:R122
- 23 31. Li D, Liu C-M, Luo R, et al. MEGAHIT: an ultra-fast single-node solution for large and
- 24 complex metagenomics assembly via succinct de Bruijn graph. Bioinformatics 2015;
- 25 31:1674–1676
- 26 32. Aguirre de Cácer D, Angly FE, Alcamí A. Evaluation of viral genome assembly and
- 27 diversity estimation in deep metagenomes. BMC Genomics 2014; 15:989
- 28 33. Roux S, Emerson JB, Eloe-Fadrosh EA, et al. Benchmarking viromics: an in silico
- 29 evaluation of metagenome-enabled estimates of viral community composition and diversity.
- 30 PeerJ 2017; 5:e3817
- 31 34. Baaijens JA, Aabidine AZE, Rivals E, et al. De novo assembly of viral quasispecies
- 32 using overlap graphs. Genome Res. 2017; 27:835–848
- 33 35. Chen J, Zhao Y, Sun Y. De novo haplotype reconstruction in viral quasispecies using
- 34 paired-end read guided path finding. Bioinformatics 2018; 34:2927–2935
- 35 36. Töpfer A, Zagordi O, Prabhakaran S, et al. Probabilistic inference of viral quasispecies
- 36 subject to recombination. J. Comput. Biol. 2013; 20:113–123
- 37 37. Prabhakaran S, Rey M, Zagordi O, et al. HIV Haplotype Inference Using a Propagating
- 38 Dirichlet Process Mixture Model. IEEE/ACM Trans. Comput. Biol. Bioinform. 2014; 11:182–
- 39 191
- 40 38. Schirmer M, Sloan WT, Quince C. Benchmarking of viral haplotype reconstruction
- 41 programmes: an overview of the capacities and limitations of currently available
- 42 programmes. Brief. Bioinform. 2014; 15:431–442
- 43 39. Said Mohammed K, Kibinge N, Prins P, et al. Evaluating the performance of tools used
- 44 to call minority variants from whole genome short-read data. Wellcome Open Res 2018;
- 45 3:21
- 46 40. Garrison E, Marth G. Haplotype-based variant detection from short-read sequencing.
- 47 arXiv [q-bio.GN] 2012;
- 48 41. Lai Z, Markovets A, Ahdesmaki M, et al. VarDict: a novel and versatile variant caller for
- 49 next-generation sequencing in cancer research. Nucleic Acids Res. 2016; 44:e108
- 50 42. Nurk S, Meleshko D, Korobeynikov A, et al. metaSPAdes: a new versatile metagenomic
- 51 assembler. Genome Res. 2017; 27:824–834
- 52 43. Simpson JT, Wong K, Jackman SD, et al. ABYSS: a parallel assembler for short read
- 53 sequence data. Genome Res. 2009; 19:1117–1123
- 54 44. Bushnell B. BBMap: a fast, accurate, splice-aware aligner. 2014;
- 55 45. Hunt M, Gall A, Ong SH, et al. IVA: accurate de novo assembly of RNA virus genomes.

1 Bioinformatics 2015; 31:2374–2376  
2 46. Yang X, Charlebois P, Gnerre S, et al. De novo assembly of highly diverse viral  
3 populations. BMC Genomics 2012; 13:475  
4 47. Zagordi O, Bhattacharya A, Eriksson N, et al. ShoRAH: estimating the genetic diversity  
5 of a mixed sample from next-generation sequencing data. BMC Bioinformatics 2011; 12:119  
6 48. Fedonin GG, Fantin YS, Favorov AV, et al. VirGenA: a reference-based assembler for  
7 variable viral genomes. Brief. Bioinform. 2019; 20:15–25  
8 49. Mikheenko A, Saveliev V, Gurevich A. MetaQUAST: evaluation of metagenome  
9 assemblies. Bioinformatics 2016; 32:1088–1090  
10 50. Li H. A statistical framework for SNP calling, mutation discovery, association mapping  
11 and population genetical parameter estimation from sequencing data. Bioinformatics 2011;  
12 27:2987–2993  
13 51. Poplin R, Ruano-Rubio V, DePristo MA, et al. Scaling accurate genetic variant discovery  
14 to tens of thousands of samples. bioRxiv 2018; 201178  
15 52. Kurtz S, Phillippy A, Delcher AL, et al. Versatile and open software for comparing large  
16 genomes. Genome Biol. 2004; 5:R12  
17 53. Lowy-Gallego E, Fairley S, Zheng-Bradley X, et al. Variant calling on the GRCh38  
18 assembly with the data from phase three of the 1000 Genomes Project. Wellcome Open  
19 Res 2019; 4:50  
20 54. Nik-Zainal S, Alexandrov LB, Wedge DC, et al. Mutational processes molding the  
21 genomes of 21 breast cancers. Cell 2012; 149:979–993  
22 55. Alexandrov LB, Nik-Zainal S, Wedge DC, et al. Signatures of mutational processes in  
23 human cancer. Nature 2013; 500:415–421  
24 56. Gehring JS, Fischer B, Lawrence M, et al. SomaticSignatures: inferring mutational  
25 signatures from single-nucleotide variants. Bioinformatics 2015; 31:3673–3675  
26 57. Howison M, Coetzer M, Kantor R. Measurement error and variant-calling in deep  
27 Illumina sequencing of HIV. Bioinformatics 2019; 35:2029–2035  
28 58. Chen S, Zhou Y, Chen Y, et al. fastp: an ultra-fast all-in-one FASTQ preprocessor.  
29 Bioinformatics 2018; 34:i884–i890  
30 59. Li H. Aligning sequence reads, clone sequences and assembly contigs with BWA-MEM.  
31 arXiv [q-bio.GN] 2013;  
32 60. Cleary JG, Braithwaite R, Gaastra K, et al. Comparing Variant Call Files for Performance  
33 Benchmarking of Next-Generation Sequencing Variant Calling Pipelines. bioRxiv 2015;  
34 023754  
35 61. Vogel F. Non-randomness of base replacement in point mutation. J. Mol. Evol. 1972;  
36 1:334–367  
37 62. Lyons DM, Lauring AS. Evidence for the Selective Basis of Transition-to-Transversion  
38 Substitution Bias in Two RNA Viruses. Mol. Biol. Evol. 2017; 34:3205–3215  
39 63. Schirmer M, Ijaz UZ, D'Amore R, et al. Insight into biases and sequencing errors for  
40 amplicon sequencing with the Illumina MiSeq platform. Nucleic Acids Res. 2015; 43:e37  
41 64. Fumagalli M. Assessing the effect of sequencing depth and sample size in population  
42 genetics inferences. PLoS One 2013; 8:e79667









Genome 1  
Genome difference  
Genome 2



reads mapped against one of the genomes



Sequencing data  
of mixture



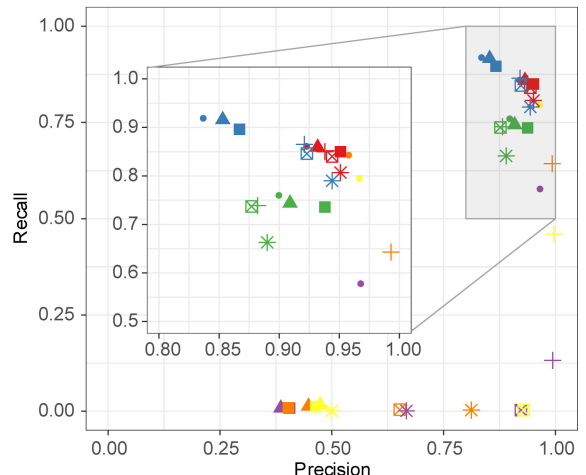
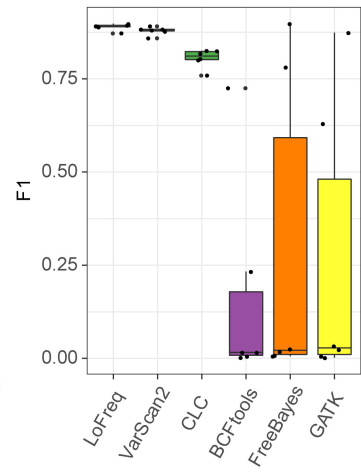
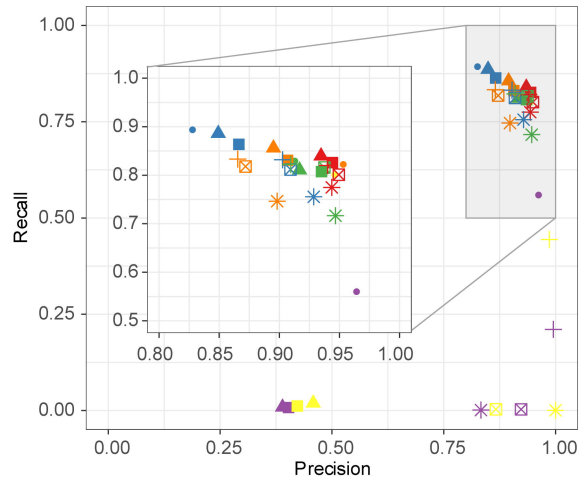
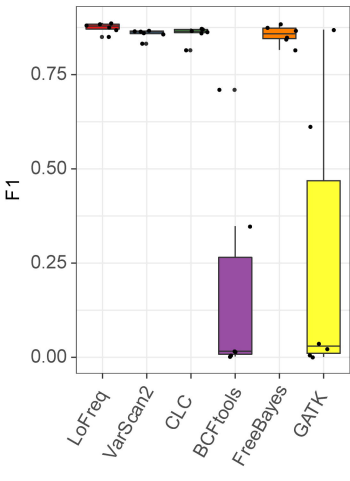
called SNPs

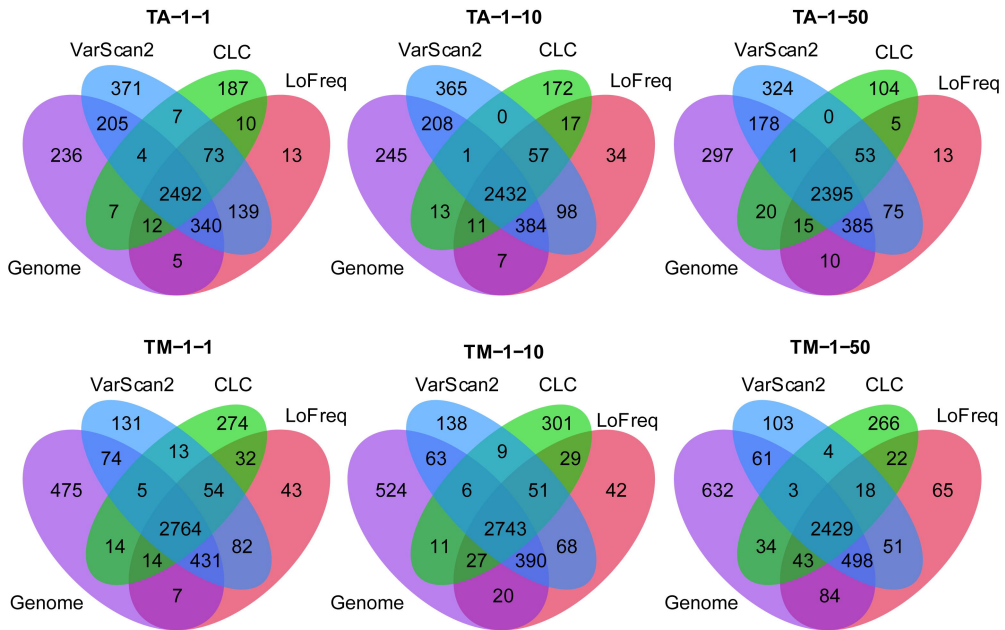


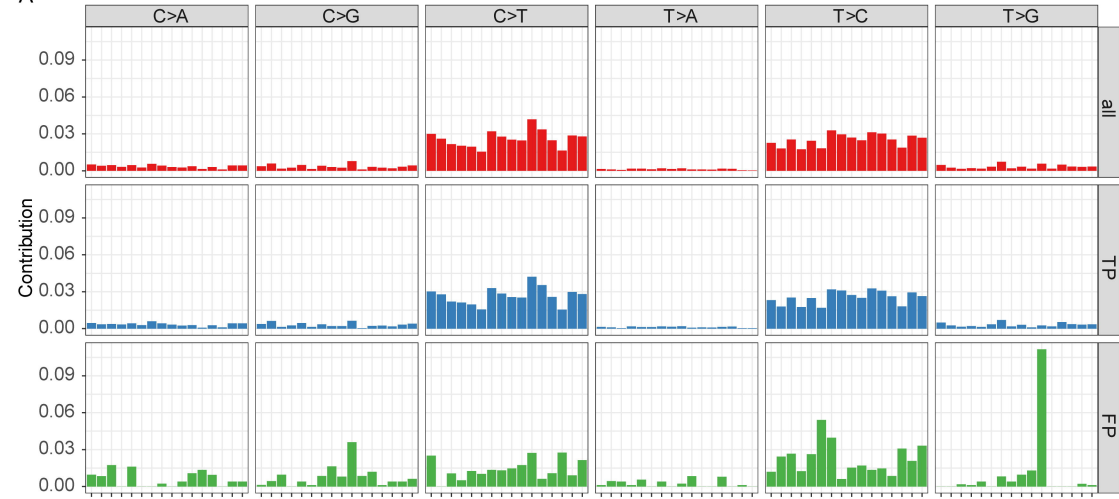
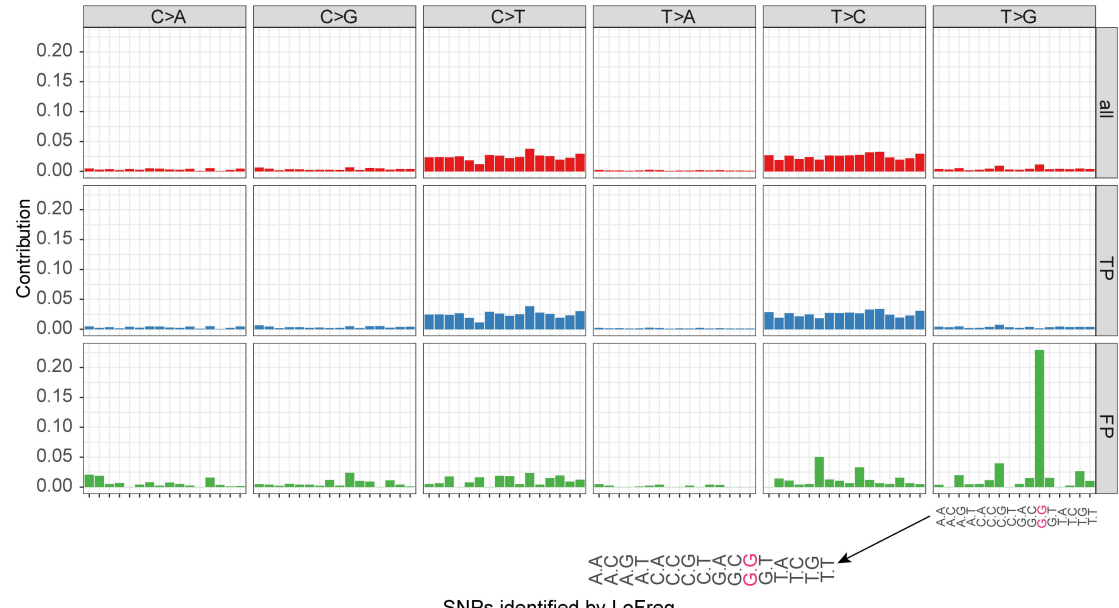
TP, FP, FN



	C	$\bar{C}$
G	TP 9	FN 2
$\bar{G}$	FP 3	

**A****B****C****D**



**A****B**

SNPs identified by LoFreq

Sequence logo showing the distribution of SNPs across the six transition types. The x-axis represents the sequence position, and the y-axis represents the contribution. The logo shows a high concentration of A and T at the first position, followed by a transition to G and C at the second position, and then a return to A and T at the third position. An arrow points from the bottom right of Panel B to this sequence logo.